Proceedings of the 40th IAHR World Congress. Rivers – Connecting Mountains and Coasts
21 – 25 August 2023, Vienna, Austria
Edited by Helmut Habersack, Michael Tritthart and Lisa Waldenberger

doi: 10.3850/978-90-833476-1-5_iahr40wc-p0090-cd

Optimal Hydraulic Design of Supercritical Bend Manholes

Gaetano Crispino[(1*)], Davide Dorthe[(2)], Corrado Gisonni[(1)] and Michael Pfister[(2)]

[(1)] Department of Engineering, Università degli Studi della Campania "L. Vanvitelli", Aversa, Italy, gaetano.crispino@unicampania.it, corrado.gisonni@unicampania.it

[(2)] Department of Civil Engineering, Haute Ecole d'Ingénierie et d'Architecture de Fribourg, Fribourg, Switzerland, david.dorthe@hefr.ch, michael.pfister@hefr.ch

Abstract

The flow pattern of supercritical bend manholes can result very complex due to the possible occurrence of the choking flow condition. This failure condition limits the maximum discharge conveyable by a bend manhole. At a design stage, it is, therefore, convenient to know the maximum capacity of the inspected bend manhole geometry and compare it to the design discharge carried out by the approach pipe. The present paper aims to give to the practitioners an immediate design tool to estimate the hydraulic capacity of supercritical bend manhole and, consequently, select the best appropriate geometrical setup. This tool consists of an empirical equation, according to which the bend manhole capacity is computed as a function of axial curvature radius, the length of the straight extension at the end of the manhole, the bend angle and the approach partial filling ratio. The accuracy was proved by carrying out a detailed experimental campaign based on the utilization of a CFD 3D numerical model.

Keywords: Bend manhole; Hydraulic design; Numerical model; Urban drainage system; Supercritical flow.

1. INTRODUCTION

Urban drainage systems are composed by channels (or pipes) and structures. The geometry of sewer channels is designed by guaranteeing that the maximum flow discharge Q_M is accompanied by an acceptable value of the partial filling ratio y. The latter should be cautiously smaller than about 0.70 to 0.75. If so, it is opportune that the corresponding mean flow velocity V_M results to be smaller than a maximum limit value, depending on the sewer infrastructure type (separate or combined) and on specific local regulations. The design relation between Q_M and y is usually taken under the assumption of the uniform flow condition. Additionally, the safe design of closed sewer conduits with stable supercritical flows (Froude number F > 2.0) requires, in principle, that choking due to the inception of hydraulic jump is avoided provided that C < 1.00 (Stahl and Hager, 1999), with C = F·y as the choking number.

Conversely, the hydraulic design of sewer structures, as sewer manholes, is often pragmatically handled. In most of the cases, recurring geometrical configurations, according to current practice, are accepted "with one's eyes closed". In other, and rare, cases, sewer manholes are designed by accomplishing empirical guidelines. For instance, Hager and Gisonni (2005) introduced specific recommendations to increase the discharge capacity of through-flow, bend and junction manholes under a supercritical flow regime. These measures were suggested to avoid the breakdown of supercritical flow, and they were conceived according to systematic observations in physical models of sewer manholes with a fixed geometrical layout. However, the realization of a sewer manhole in compliance with to these design recommendations may result onerous because the size, and consequently the total volume requirement, increases significantly. This is the case, for instance, of supercritical bend manholes, for which Del Giudice et al. (2000) and Gisonni and Hager (2002) suggested to fix an axial curvature radius R_a of three times the sewer pipe diameter D and to add a straight extension, at the end of the bend, with a length of 2D.

The design criteria by Del Giudice et al. (2000) and Gisonni and Hager (2002) are, in principle, valid for only one geometrical layout of bend manholes, which was constructed and utilized to perform the experimental tests. In this bend manhole configuration, the relative curvature radius R_a/D was always equal to 3, and the straight extension, if present, had a unique length of 2D. No evidence was proved in the laboratory for supercritical bend manholes with R_a/D < 3 or by installing a shorter straight extension at the end of the manhole. To bridge this gap, Crispino et al. (2023) have recently performed a set of numerical simulations, based on a

three-dimensional and Volume-of-Fluid model, to demonstrate how the discharge capacity of 45° and 90° supercritical bend manholes varies by changing R_a and L.

In the present paper, the numerical investigation carried out by Crispino et al. (2023) is briefly described. Then, the main results, among which a design relation to predict the discharge capacity with a variable geometry and a design chart for supercritical bend manholes, are illustrated. In the end, one practical example is proposed to individuate the specific hydraulic conditions for which the hydraulics of supercritical bends can result more restricting than across straight sewer conduits.

2. METHODOLOGY

The present study is based on the utilization of the volume of fluid (VOF) method to simulate the supercritical flow across a bend manhole with a variable geometrical configuration. The numerical modelling was conducted by using the commercial CFD software Flow 3D. In the latter, the turbulence was solved by adopting the renormalization group (RNG) *k-ε* model, which was successfully applied in several experimental investigations of hydraulic structures under a supercritical flow regime (Brown and Crookston, 2016; Azimi and Shabanlou, 2018; Huang and Wang, 2018). More details about the basic equations solved by the numerical code are presented by Crispino et al. (2023).

2.1. Experimental Setup

Based on the physical model used by Del Giudice et al. (2000) and Gisonni and Hager (2002), a numerical model of bend manhole was constructed through a CAD software. The overall structure was composed of three main elements:

i. an approach pipe, with diameter D = 0.240 m, which conveyed the supercritical flow inside the bend manhole;
ii. the bend manhole, with a U-shaped cross section characterized by a bottom semicircular cross-section half of same diameter D and two upper vertical walls of height equal to D. The plan layout of the bend was described by the axial curvature radius R_a and the bend angle θ. In some configurations, the bend manhole was extended through the addition of a L-long straight extension. If present, the latter has the same U-shaped cross-section of the bend;
iii. a downstream pipe, with diameter D.

A 3D sketch of the entire structure is represented in the Figure 1. The supercritical flow, characterized by a flow discharge Q, a water depth h_o and a Froude number

$$F_o = Q/(gh_o^4D)^{0.5} \quad [1]$$

enters the bend manhole through the approach pipe (subscript: o). The hydraulic features of the downstream flow are denoted with the subscript d, instead.

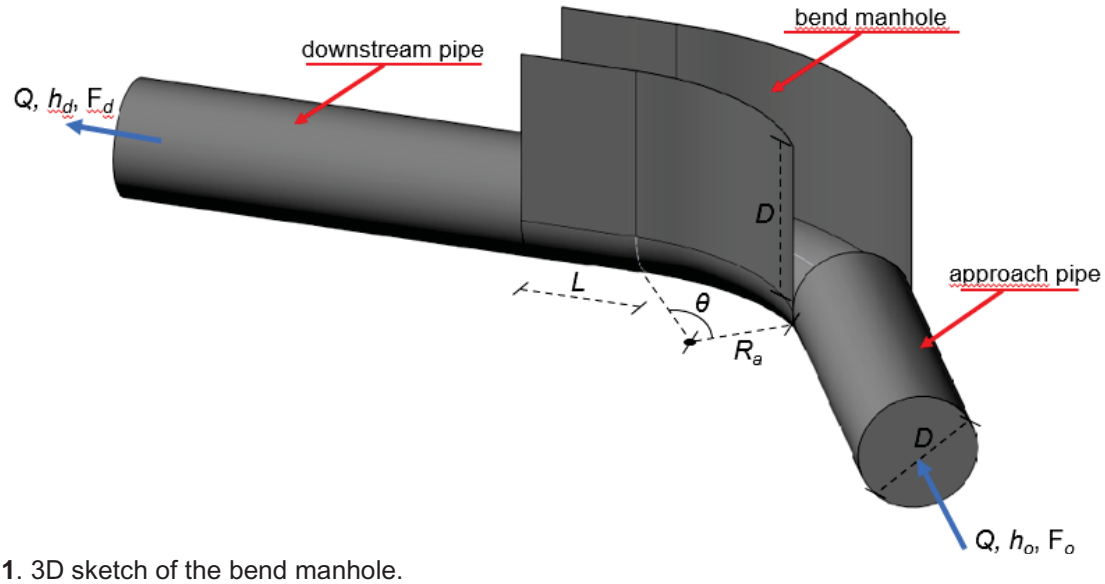

Figure 1. 3D sketch of the bend manhole.

2.2. Grid Generation and Boundary Conditions

When using a numerical model, it is opportune that the computational domain results to be similar to the physical model as much as possible. For this reason, the 3D numerical model was very close to the real

geometrical model investigated by Del Giudice et al. (2000) and Gisonni and Hager (2002). The only difference consisted in the length of the approach and downstream pipes, which were slightly shorter than in the physical model. The approach pipe was 5.3·*D*-long, whereas the length of the downstream pipe was equal to 12·*D* (manhole not equipped with the straight extension) or to 10·*D* (the straight extension was added at the end of the bend). However, the reduction of the pipe lengths did not imply the occurrence of backwater or tailwater effects.

The 3D numerical model was composed of only one single mesh block. The technology of Fractional Area-Volume Obstacle Representation (FAVOR) was adopted to define the mesh with hexahedral cells. Moreover, in this study the mesh was uniform.

The upstream boundary condition consisted in the volume flow rate condition, with a fixed fluid elevation. The latter was made equal to the uniform flow depth, according to the physical model observations collected by Del Giudice et al. (2000) and Gisonni and Hager (2002). At the downstream border, instead, a stagnation pressure condition, with a fixed value of the fractional area equal to zero, was imposed with the aim to replicate the standard free-overfall condition. On both sides and at the bottom of the domain, a standard rigid wall condition was adopted.

2.3. Numerical Model Calibration

The numerical model was calibrated by comparing a set of hydraulic features detected across the entire structure with the corresponding physical model observations by Del Giudice et al. (2000) and Gisonni and Hager (2002). The hydraulic behaviour of the bend manhole was also analyzed and set side by side with the physical model one. In particular, two calibration parameters were varied during this stage:

- the hydraulic roughness k_s of the material structure. In the physical models, the bend manholes were built of PVC whereas the material of the approach and downstream pipe along with the vertical walls of the manholes was the transparent Perspex. For this reason, k_s was alternatively set equal to 0.00 m (as for perfect smooth pipes), $1.50 \cdot 10^{-6}$ m (new plastic pipes) and $1.50 \cdot 10^{-3}$ m.
- the mesh cell dimension d_s. Three values of d_s were assumed: d_s = 0.008 m, d_s = 0.010 m and d_s = 0.012.

Three geometrical arrangements of bend manhole were retained in this phase: two of them relate to the 45° bend manhole (θ = 45°) and the third one refers to the 90° bend manhole (θ = 90°). It should be also remarked that the free-surface supercritical flow regime was preserved in all these physical model experiments. No choking was observed, therefore.

The geometrical and hydraulic characteristics of the tests carried out during the calibration phase are detailed in the Table 1. The numerical comparison was conducted with reference to:

- the maximum water depth h_M observed within the bend manhole;
- the flow depths detected along the outer side wall of the bend, at a deflection angle of 15°, 30°, 45°, 60°, 75° and 90° (the last three angles exist only for θ = 90°);
- the maximum water depth h_1 measured along the downstream pipe.

Table 1. Geometrical and main flow features of the calibration tests.

Geometry ID	θ [°]	R_a/D [-]	L/D [-]	Q [l/s]	F_o [-]	h_M [m]
I	45	3	0	9.80	2.56	0.11
				28.20	2.15	0.17
				38.90	1.90	0.26
II	45	3	2	31.00	4.78	0.27
				55.00	3.07	0.31
				67.50	1.97	0.32
III	90	3	0	18.50	5.96	0.31
				26.57	2.78	0.16

As an example, the following Figure 2 and Figure 3 show that the numerical model with d_s = 0.008 m and k_s = 0.00 m reproduced the hydraulic behaviour of the supercritical bend manhole quite accurately. All the peculiar features of the supercritical flow across the bend manhole were shown in the 3D numerical model. It was observed that the impact of the approach flow against the opposite outer wall of the manhole generated a shock wave maximum with a maximum wave depth located at a certain deflection angle δ_M. In some cases, the outer wave profile collided with the manhole end wall by provoking spray and turbulence of the free-surface. On the other hand, for the extended manhole (Geometry II, Figure 3) a secondary wave along the inner wall of the manhole occurred according to the corresponding physical evidence. In any case, the tailwater flow was rather disturbed and cross waves propagated themselves along the downstream pipe.

The accuracy of the numerical models under the different set-ups in terms of roughness and mesh cell size is shown in the plots of Figure 4. In these graphs the average relative error $\varepsilon = |p_{obs} - p_{num}|/p_{obs}$ is plotted against d_s (Figure 4a), for k_s = 0.00 m, and against k_s (Figure 4b), for d_s = 0.008 m. The average computational time t_{calc} necessary to conclude the tests is also represented. As visible, the reliability of the numerical model in the prediction of the wave depths and wave maximum increased from about 7.00 % to 11.00 % by increasing the cell size. A significant loss of precision was also found by increasing the hydraulic roughness, given that ε increased from about 7.00 % to 13.50 %. At the same time, the graphs show that t_{calc} reduced significantly if a rougher mesh was used, with a reduction factor of about 4 by passing from d_s = 0.008 m to d_s = 0.012 m. The decrease of t_{calc} was, instead, less evident when a rougher material was used.

The computational effort related to the finest mesh was retained as sustainable within this study, and for this reason the experimental program was conducted by setting d_s = 0.008 m and k_s = 0.00 m. Under this numerical set-up, the error encountered in the estimation of the observed hydraulic features is shown in the plot of Figure 5 for all the calibration tests resumed in the Table 1. Almost all the datapoints are included within the confidence range of ± 10%. The maximum errors corresponded to the calibration test with the largest value of Q (geometry II with Q = 67.50 l/s and F_o = 1.97). It is plausible that this specific experimental test was characterized by a significant amount of spray and pulsation effects in the physical model, and consequently the accuracy in the measurements of the wave depths decreased inevitably.

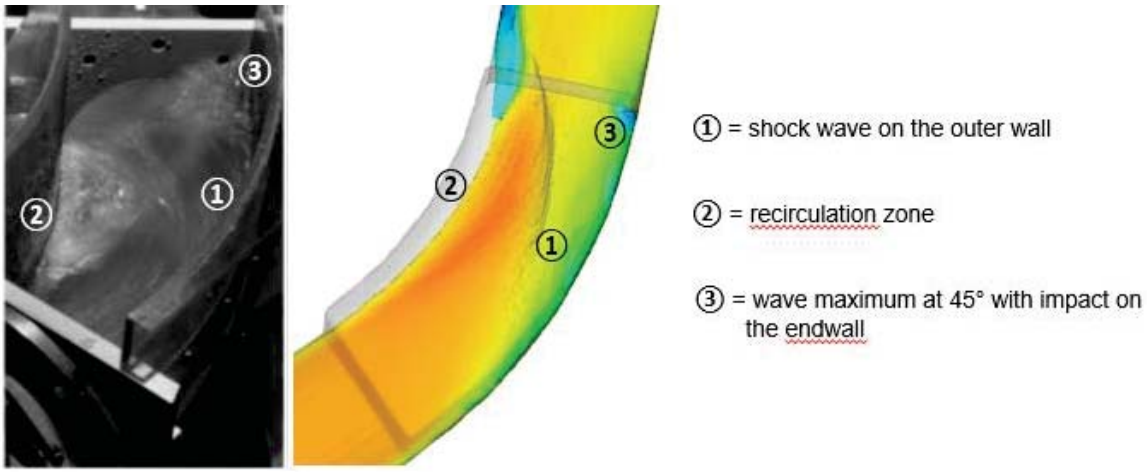

Figure 2. Geometry I, Q=38.90 l/s, F_o = 1.41: up-view of the bend manhole in operation as observed in the physical model (on the left, photograph shown in Del Giudice et al., (2000)) and in the numerical model (on the right, with d_s = 0.008 m and k_s = 0.00 m).

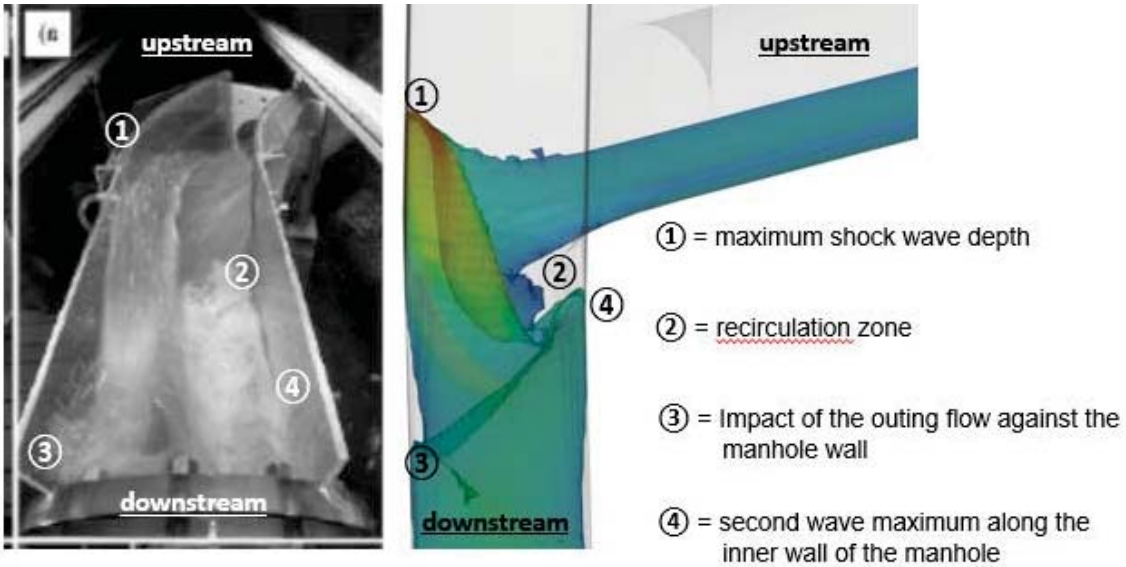

Figure 3. Geometry II, Q=31.00 l/s, F_o = 4.79: downstream view of the bend manhole in operation as observed in the physical model (on the left, photograph shown in Gisonni et al., (2002)) and in the numerical model (on the right, with d_s = 0.008 m and k_s = 0.00 m).

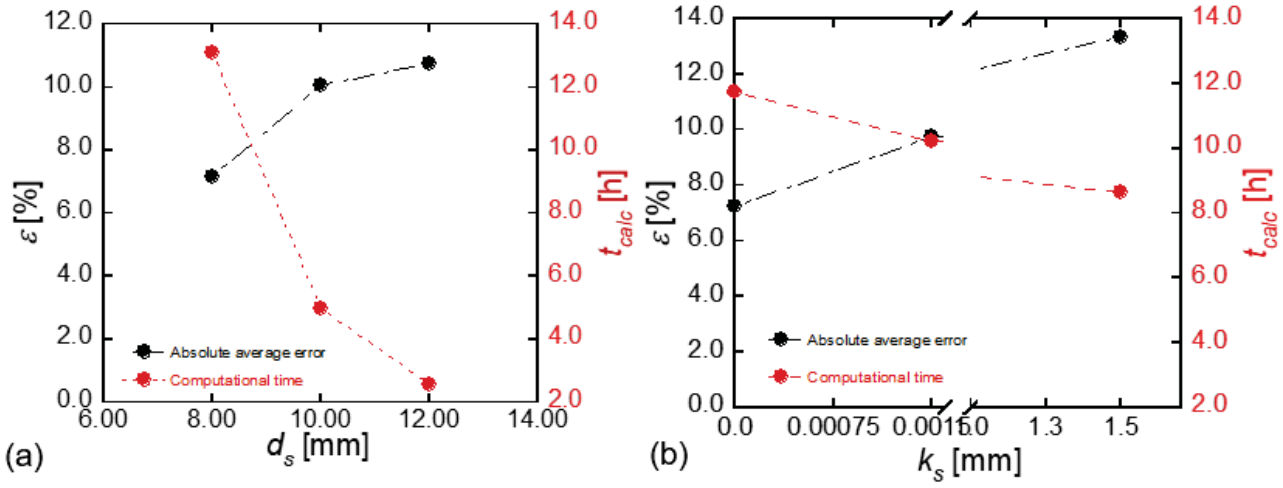

Figure 4. Relative error ε and computational time t_{calc} against: (a) cell size d_s and (b) hydraulic roughess k_s.

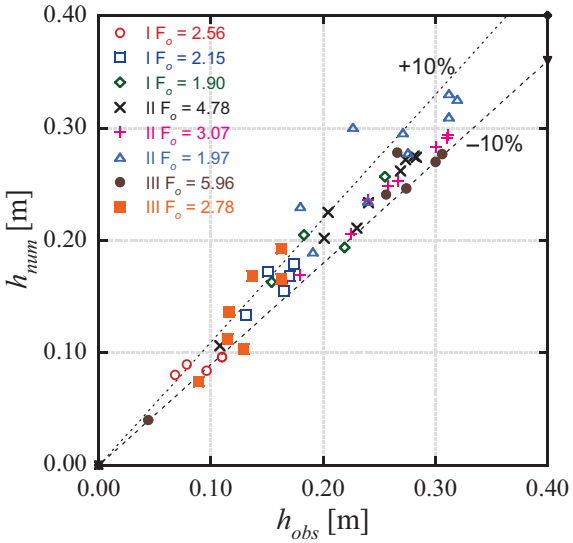

Figure 5. Comparison between observed (subscript *obs*) and numerical (subscript *num*) wave depths detected in the bend manhole and along the downstream pipe.

3. EXPERIMENTAL PROGRAM

The experimental program (Table 2) consisted in 167 tests and it was designed with the aim to investigate the effect of the variation of y_o, R_a/D and L/D on the hydraulic behaviour of supercritical bend manholes. The resulting manhole setups are listed from BM 1 to BM 11. It is noteworthy that setups BMs 8, 9 and 10 correspond to the configurations analyzed by Del Giudice et al. (2000) and Gisonni and Hager (2002).

Table 2. Experimental program.

Bend manhole setup	θ [°]	R_a/D [-]	L/D [-]	Q [l/s]	F_o [-]	y_o [m]
BM 1	45	1	0	15.91-62.48	1.30-4.00	0.30-0.60
BM 2	45	1	2	15.91-78.10	1.44-3.98	0.30-0.60
BM 3	90	1	0	15.91-62.48	1.30-4.38	0.30-0.60
BM 4	90	1	2	15.91-78.10	1.30-5.00	0.30-0.60
BM 5	45	2	0	15.91-73.92	1.30-3.85	0.30-0.60
BM 6	45	2	1	15.91-73.92	1.30-3.95	0.30-0.60
BM 7	45	2	2	15.91-78.10	1.30-5.00	0.30-0.60
BM 8	45	3	0	15.91-67.28	1.50-4.52	0.30-0.70
BM 9	45	3	2	15.91-78.10	1.50-4.85	0.30-0.70
BM 10	90	3	0	15.91-93.15	1.92-4.88	0.30-0.70
BM 11	90	3	2	15.91-103.50	1.85-5.86	0.30-0.70

For an assigned bend manhole setup, each numerical test was launched starting from the minimum Froude number for a stable supercritical flow (F_o = 1.30) and by assuming an approach filling ratio $y_o = h_o/D$ = 0.30 (upstream boundary condition). The corresponding flow discharge Q was defined by using Eq. [1]. Then, Q was progressively increased in accordance with a step-by-step hydrograph over the time. The time interval over which the discharge increased lasted 5 seconds, after which the condition with the desired value of Q was maintained for 15 seconds. This time was retained as congruous for allowing the flow regime to reach the uniform flow condition inside the structure. The discharge was increased up to achievement of the maximum value Q_C at which the manhole choked. Then, a new test was initiated by imposing a new value of y_o.

4. RESULTS

4.1. Flow Patterns of the Bend Manhole

The numerical test campaign exhibited three basic flow patterns. They are described in detail by Crispino et al. (2023) and they are synthetically defined as follows:

i. Ordinary flow pattern (Figure 6a): the supercritical enters the bend manhole and it collides against the outer wall of the structure. Consequently, a shock wave occurs whose maximum depth was, however, smaller than the wall height of the manhole. The free-surface flow regime is preserved also in the downstream pipe, along which cross waves move without generating troubling conditions for the safety of the pipe;

ii. Limit flow pattern (Figure 6b): the shock wave profile reaches the end wall of the manhole leading to the formation of a massive spray phenomenon. The outlet cross-section of the manhole results to be almost saturated and a gated flow enters the downstream pipe. The downstream filling ratio y_d is close to the maximum value allowable for a free-surface pipe flow;

iii. Failure condition (Figure 6c): The supercritical flow regime is suddenly interrupted due to the unstainable submergence of the outlet cross-section. The manhole chokes, with an alarming increase of the water level in the chamber. A hydraulic jump moves upstream by pressurizing the approach pipe. The downstream pipe is also pressurized.

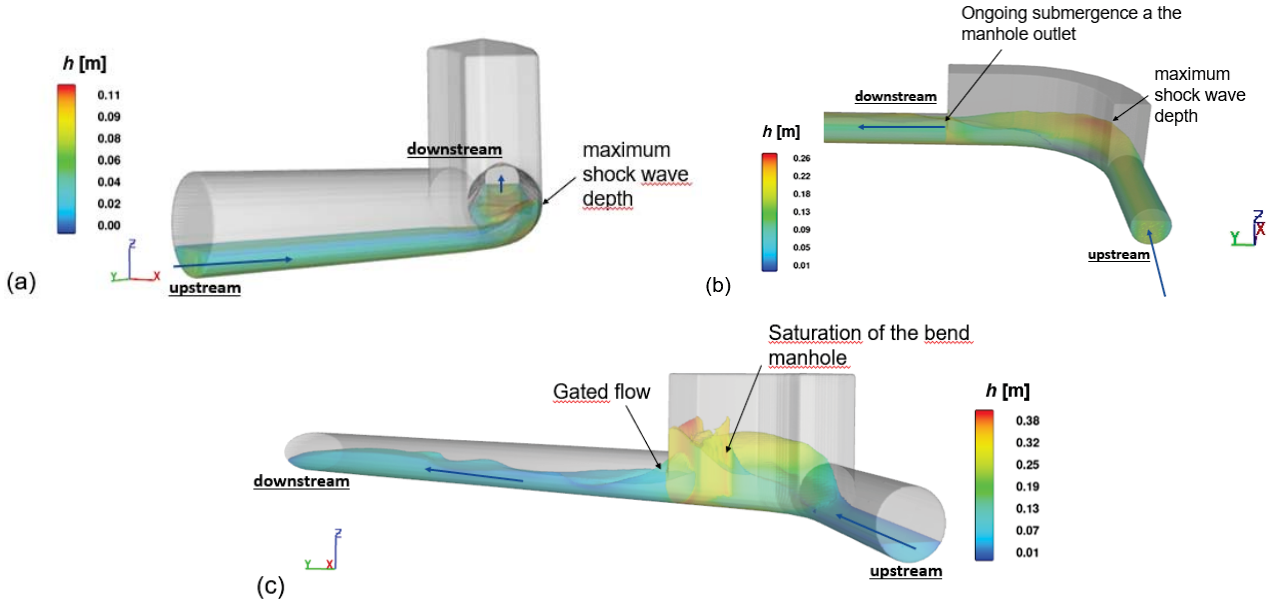

Figure 6. 3D views of the numerical model of the bend manhole under various flow patterns: (a) ordinary flow (BM 5, Q = 23.86 l/s, y_o = 0.29, F_o = 2.90), (b) limit flow (BM 11, Q = 77.63 l/s, y_o = 0.62, F_o = 1.50), (c) failure condition (BM 7, Q = 39.76 l/s, y_o = 0.35, F_o = 5.00). Blue arrows identify the flow direction.

4.2. Hydraulic Capacity

The hydraulic capacity of a supercritical bend manhole is achieved when the free-surface flow regime breaks down and, consequently, the water level increases up to saturate the manhole (choking flow). If the circumstance for which the bend manhole results to be inundated due to the backwater flow originated by the upstream shifting of a hydraulic jump along the downstream pipe, then the manhole choking is caused by the swell occurrence at the manhole outlet due to the shock wave impingement on the end wall. The flow discharge

corresponding to the achievement of the hydraulic capacity of the bend manhole is denoted as Q_C and the limit approach filling ratio at which the choking flow appears inside the manhole is y_{oC}.

In the studies of Del Giudice et al. (2000) and Gisonni and Hager (2002), Q_C is reported not dimensionally by defining the maximum capacity Froude number

$$F_{oC} = Q_C/(gD^2h_o^3)^{0.5} \quad [2]$$

Table 3 resumes the main formula and recommendations which were suggested for 45° and 90° bend manholes with R_a/D=3 and, eventually, L/D = 2.

Table 3. Empirical formula recommended by Del Giudice et al. (2000) and Gisonni and Hager (2002).

	Del Giudice et al. (2000)	Gisonni and Hager (2002)
MANHOLE TYPE	45° and 90° bend manhole	45° bend manhole
FLOW IMPROVING APPURTENANCES	Cover plate	2D straight extension and cover plate
MANHOLE CAPACITY	$F_{oC} = 3\cdot\text{sen}\theta(1 - y_o) + y_o$	$F_{oC} = 3 - 2y_o$ with straight extension $F_{oC} = 7.5\cdot(1 - y_o) + y_o$ with straight extension and cover plate
LIMIT APPROACH FILLING RATIO	y_{oC} = 0.70 for θ = 45° y_{oC} = 0.55 for θ = 90°	y_{oC} = 0.66

Figure 7 shows the variation of y_o with F_{oC} for all manhole setups analyzed in the present experimental program. The capacity of 45° bend manholes is smaller than for 90° bend manholes. The addition of the straight extension is proved to be largely effective to increase the discharge capacity of the structure. Conversely, the increase of the axial curvature radius is equally influential in the augmentation of the maximum discharge conveyable in the bend manhole, especially when R_a/D increases from 2 to 3. However, even for θ = 90°, R_a/D = 3 and L/D = 2 (BM 11), F_{oC} remains smaller than for the bend manholes equipped with the cover plate and the straight extension. The latter configuration was investigated by Gisonni and Hager (2002) and it remains the most incisive measure to increase F_{oC}.

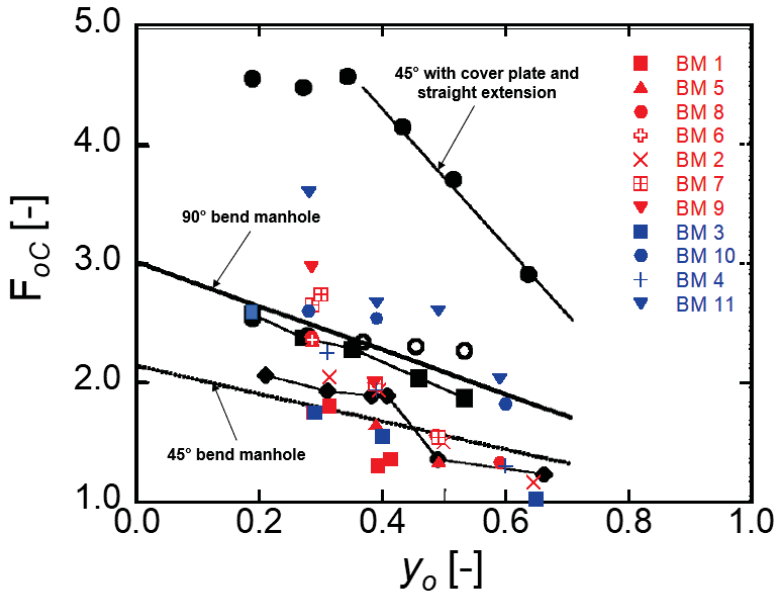

Figure 7. Capacity Froude number F_{oC} as a function of the approach filling ratio y_o for 45° and 90° bend manholes under variable geometrical setups. The black markers and lines are as illustrated in the Figure 8d of Gisonni and Hager (2002).

The analysis of the numerical data related to the limit flow pattern occurrence allowed to introduce a new empirical relation to predict F_{oC} as a function of the geometrical parameters R_a/D, L/D and θ along with y_{oC}, as follows:

$$F_{oC} = k \cdot y_{oC}^{(\alpha - 1.5)} \qquad [3]$$

with $k = 0.1 \cdot (R_a/D + L/D + 5)$ and $\alpha = 0.7 - \sin(\theta/8)$. Please note that the bend angle should be quantified in radians in the Eq. [2]. The latter can be applied in the experimental range shown in Table 2. Figure 8 provides a direct comparison between the observed (in the numerical model or in the physical models if the datapoints of Del Giudice and Hager (2000) and Gisonni and Hager (2002) are retained) and the computed (via the application of Eq. [2]) values of F_{oC}. As shown, almost all the datapoints are included between the confidence interval of ± 5%, and the overall correlation coefficient R^2 was equal to 0.92. The latter reduces to 0.62 if the former equations (as indicated in Table 3) provided by Del Giudice et al. (2000) and Gisonni and Hager (2002) are applied.

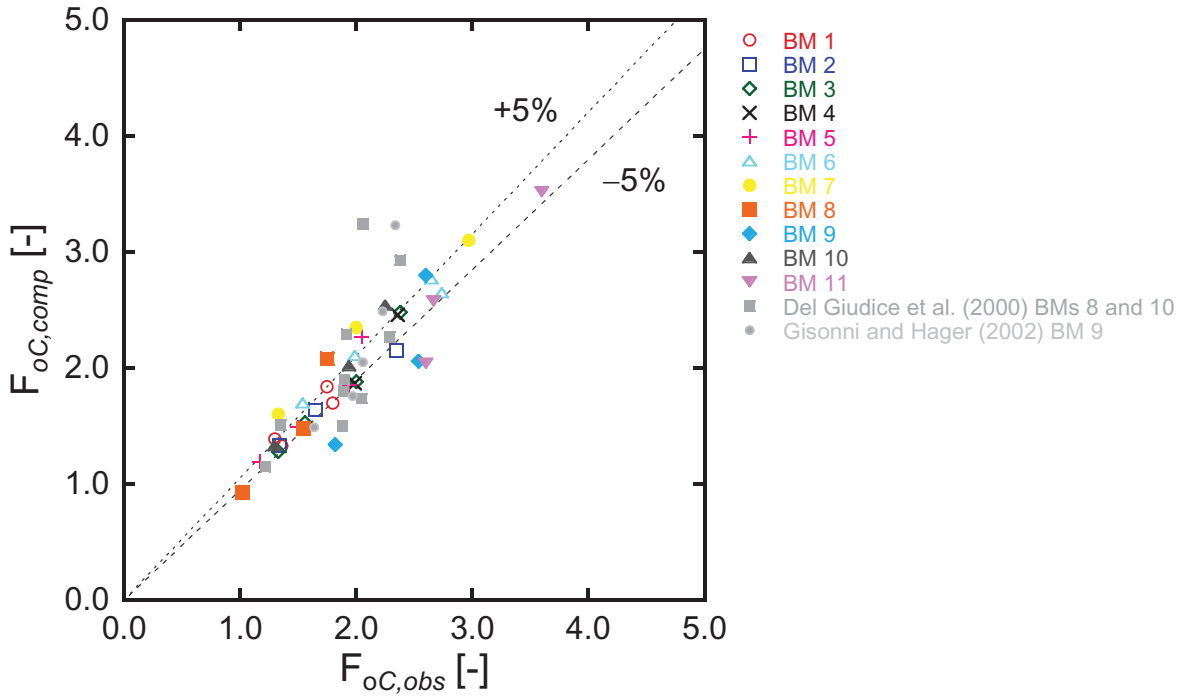

Figure 8. Comparison between observed (subscript *obs*) and computed (subscript *comp*, via Eq. [2]) values of F_{oC}.

Eq. [2] can be applied to design bend manholes across sewer collectors. At this regard, the following example illustrates a practical case-study for which the results of the present investigation are useful for performing the optimal design of such structures.

It is given a sewer plastic pipe with D = 0.50 m and a bottom slope of 2%. The uniform flow is supercritical, with the Froude number F roughly equal to 2.0. According to many local guidelines, the pipe filling ratio y should be limited to y_M = 0.75 to avoid the pipe obstruction by solid matter. This implies that the maximum flow discharge Q_M conveyable across the pipe is equal to 0.57 m^3/s (plastic pipe with Manning's roughness coefficient n = 0.0125 $sm^{-1/3}$ as suggested in ASCE, (1969)). $F_{oM} = Q_M/(gD^5y_M^3)^{0.5}$ results to be equal to 1.59, consequently. If a bend angle of 60° should be realized along the sewer line of the present pipe, then it is possible to use Eq. [2] to calculate the maximum capacity of this bend manhole prior to the occurrence of the manhole choking. Figure 9 reports the curves $F_{oC}(y_{oC})$ for a bend manhole with R_a/D = 2 and variable values of L/D. As shown, the hydraulic behaviour of the bend manhole aggravates further the design criteria to be respected for safety. It would be necessary, indeed, the addition of a straight 5D-long extension at the end of the bend manhole to preserve a safe passage of the maximum discharge with y_M = 0.75. If the straight extension length is limited to 2D, as suggested in the literature, then F_{oC} = 1.18 corresponding to a discharge Q_{oC} = 0.42 m^3/s (25% smaller than Q_M). For a bend manhole without straight extension, Q_{oC} is even reduced to 0.33 m^3/s (42% smaller than Q_M). On the other hand, Q_M might safely run across the bend manhole by limiting the approach filling ratio y_{oC} to a value ranging between 0.42 (L/D=0) and 0.55 (L/D=2). However, this would imply the installation of the bend cover at the entrance of the manhole, with additional maintenance responsibilities.

In the plot of Figure 9 there are also represented the curves derived from the design criteria for straight free-surface flows (Stahl and Hager, 1999) and bend channels (Kolarevic et al., 2015). These curves were obtained as follows. Stahl and Hager (1999) prescribed to avoid the choking flow for supercritical flows with $1 > F_o > 2$ by limiting the choking number $C = F \cdot y$ to 1.0. If the choking number definition is combined with Eq. [2], then the following criterion is obtained:

$$F_{oC} \cdot y_{oC}^{0.5} < 1.0 \quad [4]$$

Kolarevic et al. (2015) defined the threshold value of C at the transition between helical (cross waves) and choking flow along free-surface flow bends. This limit value was calculated as a function of R_a/D, y and θ as follows:

$$C = c_2 \cdot (y)^{1-c_1} \quad [5]$$

with $c_1 = 1.5 \cdot (D/R_a \sin\theta)^{0.38} + 4/3 \cdot$ and $c_2 = 0.48 \cdot (D/R_a \sin\theta)^{-0.45}$. The addition of Eq. [2] into Eq. [5] leads to:

$$F_{oC} < c_2 \cdot (y_{oC})^{2(1-c_1)} \quad [6]$$

Eq. [6] should be respected to prevent the choking flow into bend pipes according to Kolarevic et al. (2015). As visible in Figure 9, the design criterion by Kolarevic et al. (2015) is more restrictive than all the others. If $y_o < 0.40$, than the maximum capacity of a straight sewer pipe along which no choking occurs is smaller than the maximum discharge running across the 60° bend manhole with $R_a/D = 2$ placed along the same pipe. Conversely, the failure criteria of the bend manhole can be more limiting than the straight pipe choking criterion of Stahl and Hager (1999) for $y_o > 0.40$.

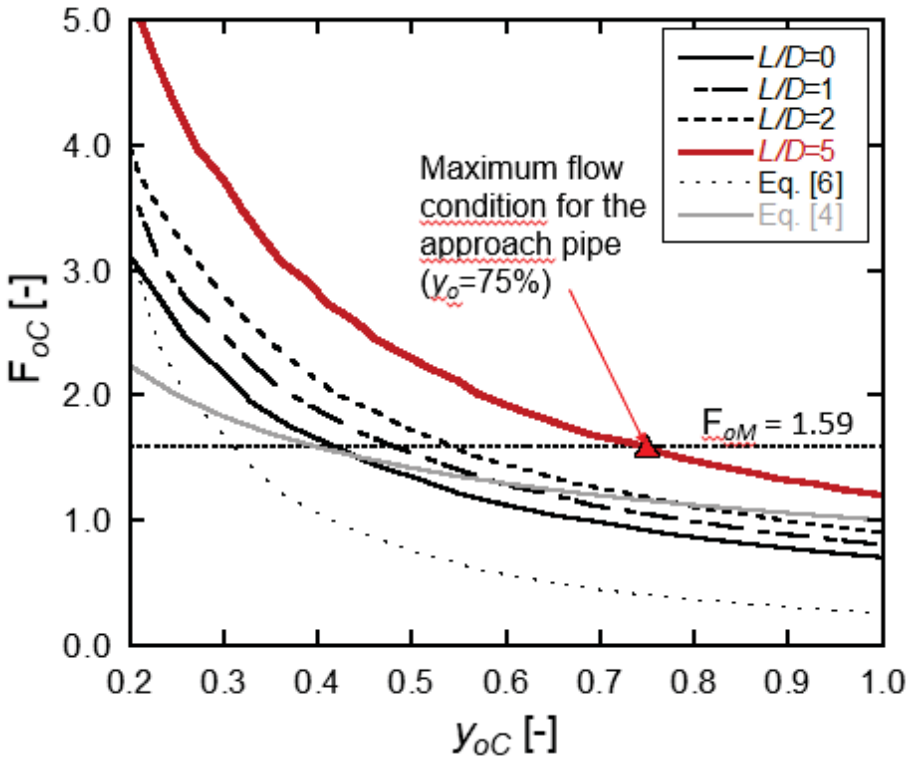

Figure 9. F_{oC} against y_{oC} for a supercritical 60° bend manhole with $R_a/D = 2$.

5. CONCLUSIONS

In the present paper supercritical bend manholes were studied with the aim to provide design criteria for such sewer structures. A 3D numerical investigation, based on the of the volume of fluid method and on the assumption of the renormalization group (RNG) k-ε turbulence model, was carried out through the utilization of the CFD commercial software FLOW 3D.

The numerical model reproduced the basic geometry of bend manholes which was previously examined by Del Giudice et al. (2000) and Gisonni and Hager (2002). The data of the latter experimental campaigns were used to calibrate the numerical model. In particular, the measurements of the wave depths observed along the outer wall of the manhole along with the maximum water depths inside the structure and along the downstream pipe represented the comparison term with the corresponding data extracted by numerical models with variable roughness coefficients and mesh cell sizes.

After the calibration, a large set of numerical tests was carried out to define the effect of the main geometrical and hydraulic parameters on the maximum capacity of supercritical bend manholes. The numerical data related to the limit flow conditions before the occurrence of the manhole choking were specifically analyzed to derive a new equation for predicting the bend manhole capacity. Similarly to Del Giudice et al. (2000) and Gisonni and Hager (2002), a not dimensional parameter, namely the maximum capacity Froude number, was selected to define the maximum capacity. This parameter was demonstrated to be accurately computable as a function of the axial curvature radius, the length of the straight extension, the bend angle and the approach partial filling ratio. It was also proved that the herein proposed equation provides more accurate estimates than the former relations by Del Giudice et al. (2000) and Gisonni and Hager (2002) for 45° and 90° supercritical bend manholes.

At the end of the paper, a numerical example based on the application of the design criteria for straight and bend sewer pipes (Stahl and Hager, 1999; Kolarevic et al., 2015) and on the new equation for supercritical bend manholes was proposed with reference to a 60° bend manhole with an assigned axial curvature radius. The results showed that, in some cases, the conditions to respect to prevent the occurrence of the choking within supercritical bend manholes are more restricting than that ones for straight flow pipes.

6. ACKNOWLEDGEMENTS

The authors acknowledge the financial support of the Swiss Federal Office for the Environment (BAFU-087.2-527/287/3) and of CREABETON PRODUKTIONS AG (Switzerland). Its representative, Thomas Rohr, gave much practical advice. This work was also supported by the special funding “Progetto Giovani Ricercatori” released by Università degli Studi della Campania “L. Vanvitelli”. Thank you!

7. REFERENCES

American Society of Civil Engineers ASCE (1969). Design and construction of sanitary and storm sewers. *Manuals and Reports of Civil Engineering Practise*, 37, ASCE: New York.

Azimi, H., and Shabanlou, S. (2018). Numerical study of bed slope change effect of circular channel with side weir in supercritical flow condition, *Applied Water Science*, 8 (166), https://doi.org/10.1007/s13201-018-0816-5.

Brown, W.K., and Crookston, B.M. (2016). Investigating supercritical flows in curved open channels with three dimensional numerical modelling. *6th International Symposium on Hydraulic Structures: Hydraulic Structures and Water System Management, ISHS 2016*, Ed. B.M. Crookston and B.P. Tullis, Portland, OR, 213-222.

Crispino, G., Dorthe, D., Gisonni, C., and Pfister, M. (2023). Hydraulic capacity of bend manholes for supercritical flow, *Journal of Irrigation and Drainage Engineering*, 149 (2), 04022048.

Del Giudice, G., Gisonni, C., and Hager, W.H. (2000). Supercritical flow in bend manhole. *Journal of Irrigation and Drainage Engineering*, 126 (1), 48-56.

Gisonni, C., and Hager, W.H. (2002). Supercritical flow in manholes with a bend extension. *Experiments in Fluids*, 32 (3), 357-365.

Hager, W.H., and Gisonni, C. (2005). Supercritical flow in sewer manholes. *Journal Hydraulic Research* 43 (6), 659-666.

Huang, X.-b., and Wang, Q. (2018). Numerical models and theoretical analysis of supercritical bend flow, *Water Science and Engineering*, 11 (4), 338-343.

Kolarevic M., Savic L., Kapor R., Mladenovic N. (2015). Supercritical flow in circular conduit bends. *Journal of Hydraulic Research*, 53 (1), 93-100, https://doi.org/10.1080/00221686.2014.932856.

Stahl, H., and Hager, W.H. (1999). Hydraulic jump in circular pipe. *Canadian Journal of Civil Engineering*, 26, 368-373, https://doi.org/10.1139/l98-068.